JQS Journal of Quaternary Science QRA

Rapid climate changes during the Lateglacial and the early Holocene as seen from plant community dynamics in the Polar Urals, Russia

ANNE E. BJUNE,[1]* INGER GREVE ALSOS,[2] JO BRENDRYEN,[3] MARY E. EDWARDS,[4] HAFLIDI HAFLIDASON,[3] MAREN S. JOHANSEN,[5] JAN MANGERUD,[3] AAGE PAUS,[5] CARL REGNÉLL,[3] JOHN-INGE SVENDSEN[3] and CHARLOTTE L. CLARKE[4]

[1]Department of Biological Sciences and Bjerknes Centre for Climate Research University of Bergen, Bergen, Norway
[2]The Arctic University Museum of Norway, UiT – The Arctic University of Norway, Tromsø, Norway
[3]Department of Earth Science and Bjerknes Centre for Climate Research University of Bergen, Bergen, Norway
[4]School of Geography and Environmental Science, University of Southampton, Highfield, Southampton, UK
[5]Department of Biological Sciences, University of Bergen, Bergen, Norway

ABSTRACT: A detailed, well-dated record of pollen and sedimentary ancient DNA (*sed*aDNA) for the period 15 000–9500 cal a BP describes changes at Lake Bolshoye Shchuchye in the Polar Ural Mountains, located far east of the classical Lateglacial sites in western Europe. Arctic tundra rapidly changed to lusher vegetation, possibly including both dwarf (*Betula nana*) and tree birch (*B. pubescens*), dated in our record to take place 14 565 cal a BP, coincident with the onset of the Bølling in western Europe; this was paralleled by increased summer temperatures. A striking feature is an early decline in *Betula* pollen and *sed*aDNA reads 300 years before the onset of the Younger Dryas (YD) in western Europe. Given the solid site chronology, this could indicate that the YD cooling started in Siberia and propagated westwards, or that the vegetation reacted to the inter-Allerød cooling at 13 100 cal a BP and did not recover during the late Allerød. During the YD, increases in steppe taxa such as *Artemisia* and Chenopodiaceae suggest drier conditions. At the onset of the Holocene, the vegetation around the lake reacted fast to the warmer conditions, as seen in the increase of arboreal taxa, especially *Betula*, and a decrease in herbs such as *Artemisia* and Cyperaceae. © 2021 The Authors *Journal of Quaternary Science* Published by John Wiley & Sons Ltd.

KEYWORDS: Lateglacial vegetation and climate; Polar Ural Mountains; pollen; sedimentary ancient DNA

Introduction

The Last Glacial–Interglacial Transition (LGIT), about 15 000–11 000 calibrated years before the present (cal a BP), is characterized by major climate changes: the Bølling (warm) – Older Dryas (OD, cold) – Allerød (warm) – Younger Dryas (YD, cold) intervals (Mangerud *et al.*, 1974). These oscillations were first described from Scandinavia (Mangerud, 2021) and later recognized around much of the globe, although often with different climate responses; this is especially so for the YD. The largest amplitudes of temperature change occurred in the area from Greenland through north-west Europe and intermediate latitudes around the North Atlantic Ocean. They are presumed to be the result of major changes in sea-ice cover in the Nordic Seas (Sadatzki *et al.*, 2019). Less clear is how climate changes that are strongly linked to the North Atlantic and adjacent lands propagated eastwards into the Eurasian continental landmass.

An abrupt warming took place in western Europe at the onset of the Bølling, and it lasted, with small interruptions, including the OD, through the Allerød until the onset of the YD. The onset of the Bølling is dated to 14 692 b2k (14 642 cal a BP) in the Greenland ice cores and this abrupt transition is estimated to have occurred over 3 years (Rasmussen *et al.*, 2006). According to Brendryen *et al.* (2020), the ice sheet in the Barents Sea disappeared completely within a few hundred years during the Bølling. The YD is the most recent major climate oscillation; it is seen in northern Europe as a cold (and dry) period that interrupted the gradual warming trend after the LGM. The onset of the YD and the impact of this abrupt climate change on vegetation is seen in many studies; however, variations in the nature of those vegetation changes within the YD stadial itself – and their exact timing – are often not discussed. This is probably due to low sampling resolution and/or the lack of robust age models in many studies (Muschitiello and Wohlfarth, 2015; Tarasov *et al.*, 2021).

The Ural Mountains and adjacent areas comprise an attractive region for studying vegetation responses to climate change during the Lateglacial because much of the region remained ice-free during the Last Glacial Maximum (LGM) around 23 000–19 000 cal a BP (Fig. 1, inset), apart from some small mountain glaciers (Mangerud *et al.*, 2008; Svendsen *et al.*, 2019). In this study, we present results from Lake Bolshoye Shchuchye (67.89°N, 66.35°E; 187 m a.s.l.), located in the northernmost part of the Ural Mountains. The lake catchment has probably been without any large glaciers for at least 60 000 years (Mangerud *et al.*, 2002, 2008; Hughes *et al.*, 2016; Svendsen *et al.*, 2019;). Only a handful of earlier palaeoecological studies from the vicinity of the Ural Mountains span the Lateglacial period (Paus *et al.*, 2003; Väliranta *et al.*, 2006; Clarke *et al.*, 2020; Tarasov *et al.*, 2021). Binney *et al.* (2017) describe the most prominent vegetation responses since the LGM as changes in pollen-based biome distributions that reflect dominant plant functional types (PFTs) across the Eurasian continent. They show that west of 40°E (the White Sea) there is a decrease in woody PFTs centred on the 12.5 (13–12) cal ka time slice, whereas east of 40°E there is no

*Correspondence: A. E. Bjune, as above.
E-mail: anne.bjune@uib.no

Figure 1. Location of the study site at Lake Bolshoye Shchuchye and its smaller sister Lake Maloye Shchuchye, in the Polar Ural Mountains of Arctic Russia. The dashed white line indicates the hydrological catchment of our study lake. The red dot indicates the location where the sediment cores (506-48 and 506-50) analysed for pollen and *sed*aDNA were taken. Numbers indicate the altitude of the highest mountain peaks within the lake's catchment. Inset map shows the ice sheet limit during the Last Glacial Maximum (bold white line) from Svendsen *et al.* (2004) and the present-day boreal tree line (black dashed line). Redrawn from Clarke *et al.* (2020). [Color figure can be viewed at wileyonlinelibrary.com]

clear signal of the YD. The predominance of open arctic–alpine vegetation following the LGM until the onset of the Holocene is shown in several studies in the Polar Urals and nearby regions (Andreev *et al.*, 2004; Svendsen *et al.*, 2014; Clarke *et al.*, 2020).

Glacial varves and a fast sedimentation rate in Lake Bolshoye Shchuchye indicate that there were glaciers in the catchment from 24 000 to 18 700 cal a BP (Regnéll *et al.*, 2019; Svendsen *et al.*, 2019). From 18 700 cal a BP the sedimentation rate gradually decreased and varves became progressively less frequent, disappearing completely after the start of the Bølling. Apparently, the glaciers disappeared completely from the catchment at around 14 350 cal a BP, and there is nothing to suggest that new glaciers formed during the YD (Regnéll *et al.*, 2019; Svendsen *et al.*, 2019).

The complete vegetation history covering the last 24 000 years from Lake Bolshoye Shchuchye is presented in Clarke *et al.* (2020), using pollen, spores and sedimentary ancient DNA (*sed*aDNA) from the full 24-m-long core (core no. 506-48). Constraints arising from the nature of vegetation proxy data, such as differential rates of production, reproduction, representation and preservation, plus response times to environmental change can limit the ability to reconstruct detailed vegetation histories. For example, low pollen production is a characteristic feature of the open arctic–alpine landscape that dominated much of northern Eurasia during the LGM until the start of the Holocene. At Lake Bolshoye Shchuchye, however, both pollen and *sed*aDNA have exceptionally good preservation and show a taxonomically rich record of vegetation change (Clarke *et al.*, 2020), and their use in combination gives a more complete view of vegetation dynamics.

The long record of Clarke *et al.* (2020) lacks detailed temporal resolution. In this paper we present an updated version for the period 15 000–9500 cal a BP that features more radiocarbon dates and a much denser sampling for pollen and *sed*aDNA analysis; this provides exceptionally high temporal resolution (mean of 80 years per sample). This study aims to utilize the high-resolution data to increase the understanding of the rapid vegetation changes and the climatic implications during the selected time interval.

Geographical, geological and vegetational setting

Lake Bolshoye Shchuchye is the largest (~13 km long and ~1 km wide) and deepest (~140 m) lake in the Polar Urals, the northernmost section of the Ural Mountain chain (Fig. 1). The lake was formed by glacial erosion and follows weaknesses along the ancient NW–SE-striking faults. Details on the lake formation, lake development and landscape processes are described in earlier publications (Haflidason *et al.*, 2019a,b; Regnéll *et al.*, 2019; Svendsen *et al.*, 2019). The lake has a catchment area of 215 km², with a deltaic inlet at its northern shore formed by the Paiatanyu River and an outlet at its southern end draining into the Bolshoye Shchuchya River, a tributary of the Ob River. High mountain peaks and steep-sided valley slopes surround the lake, with elevations reaching 500–1100 m a.s.l. at its north-western shore.

Present-day climate conditions are characterized as cold and continental, with a mean summer temperature (June–July-August) of 7 °C at Bolshaya Khadata, located at 260 m a.s.l. some 25 km to the south of Lake Bolshoye Shchuchye. The vegetation around the lake is for the most part a low-growing

tundra mosaic, comprising grasses, dwarf shrubs, sedges, mosses and lichens. Patchy thickets of green alder (*Alnus viridis*) grow on south-facing slopes up to an elevation of around 300 m a.s.l. The lake lies north of the regional treeline, and there are no other trees growing within the catchment today (Fig. 1). At higher elevations, the vegetation is discontinuous with exposed rocky surfaces supporting alpine grass and forb communities. Clarke *et al*. (2019) provide a record of all taxa observed in the *seda*DNA data and a floristic comparison with the present-day vegetation based on surveys and literature. They show that virtually all taxa in the *seda*DNA record are present in the area surrounding the lake, if not in the actual catchment.

Methods

Sediments and age model

We use data from two parallel ca. 24-m-long sediment cores (core numbers 506-48 and 506-50) retrieved from the southern end of Lake Bolshoye Shchuchye, which span the last ca. 24 000 years. Full details of the study site (Fig. 1), coring and field work are provided by Svendsen *et al*. (2019).

The cores have been stored at 4 °C since collection in 2009. They were split longitudinally in 2014 to retrieve sub-samples for radiocarbon dating. The cores remained in cold storage until subsampling for pollen and *seda*DNA in 2015 and 2019, respectively. Sub-samples for pollen and *seda*DNA were taken from the same depths where possible.

Detailed sediment descriptions and the previously used chronology of each core can be found in Regnéll *et al*. (2019) and Svendsen *et al*. (2019). The radiocarbon dates are based on small (<1-mm-diameter) and unidentifiable plant fragments (Svendsen *et al*., 2019), thus avoiding any lake reservoir effect. In this study, we predominantly use samples from core 506-48, but a 20-cm-long gap between two core sections at 593 cm was spliced with material from the parallel core (506-50). All data and figures presented in this paper use the composite depth scale after this splicing, which differs slightly from the depth scales used in earlier papers on Lake Bolshoye Shchuchye.

For the chronology, we use the new IntCal20-calibration curve for ^{14}C ages (Reimer *et al*., 2020). The terminology of chronozones follows Mangerud (2021).

The new age–depth model (Fig. 2) is constructed by Bayesian depositional modelling using OxCal 4.4.1 (Bronk Ramsey, 2009a) and calibrated using the IntCal20 calibration curve (Reimer *et al*., 2020). In this paper we focus on the time interval between 15 000 and 9500 cal a BP; the completely new age model for the whole core is presented in Haflidason *et al*. (this issue). The age–depth model for the entire core (Fig. 2) is based on 27 samples of terrestrial macrofossils dated by ^{14}C accelerator mass spectrometry (AMS) (Haflidason *et al*., this issue), the Vedde Ash (Haflidason *et al*., 2019a), and counting of a floating sequence of about 5000 annual laminations (varves) in the lower 1260 cm of the core (Regnéll *et al*., 2019). The calendar age of the Vedde Ash (median: 12 050 cal a BP, 95% range: 12 142–11 946 cal a BP) is from Lohne *et al*. (2014), recalibrated with IntCal20.

For age-model construction, we used the OxCal P_Sequence depositional model (Bronk Ramsey, 2008). Boundary commands were inserted at transitions where the sediment stratigraphy indicates changes in the sedimentation pattern, thus creating changes in sedimentation rate. We used the variable *k* option (Bronk Ramsey and Lee, 2013) to estimate objectively how variable the sedimentation rate could be

between dated samples. Each ^{14}C date was tested for being an outlier with the general outlier model (Bronk Ramsey, 2009b), assuming a prior probability of 5% for a date to be an outlier. Resulting outliers were down-weighted in the depositional model. Even when down-weighted in the analysis, some of the dates that are flagged as outliers still exert an influence on the final age model. As a sensitivity test for the choices regarding outliers, we constructed an alternative age model where we excluded dates that had a probability of more than 5% for being an outlier. The alternative age model is shown in Supporting Information Figure S1. The two age models agree well within their credible intervals. The most prominent differences between the two are that the alternative model shows slightly younger ages in the first part of the YD, and slightly older ages at the end of the YD and during the early Holocene.

Pollen samples

In total, 148 pollen samples have been analysed from cores 506-48 and 506-50 (Clarke *et al*., 2020). Here we use 69 pollen samples from the time interval 9500–15 000 cal a BP (385–716 cm; equal to zones BS2–BS4 in Clarke *et al*., 2020). Thirty additional subsamples of 1.0 or 0.5 cm^3 were prepared using standard methods (acetolysis and HF; Fægri and Iversen, 1989) and were mounted in glycerol. Two to four *Lycopodium* spore tablets (*n* = 18 584) were added to each sample to calibrate pollen concentration. Where possible, at least 300 pollen grains of terrestrial taxa were identified per sample using taxonomic keys (Fægri and Iversen, 1989; Beug, 2004) and an extensive reference collection at the Department of Biological Sciences, University of Bergen, Norway. The pollen sum (ΣP) includes all terrestrial pollen and spore taxa, thus excluding aquatic taxa.

Pollen percentage and pollen influx diagrams were drawn using the Tilia and TGView software (Grimm, 2011; tiliait. com). The pollen diagram was subdivided into local pollen assemblage zones using a stratigraphically constrained cluster analysis on pollen percentage data by sum-of-squares (CON-ISS), as developed by Grimm (1987). The number of usable zones was determined by comparison with the broken-stick model (Bennett, 1996; Birks, 1998) using the vegan (Oksanen *et al*., 2017) package for R (R Core Team, 2017).

Betula pollen size measurements

Betula pollen size (grain diameter and pore depth) was measured using a light microscope with an attached Axio camera using a 60× objective and immersion oil. Calculations of grain diameter: pore-depth ratio follow the description in Birks (1968). According to Birks (1968) pollen grains of dwarf birch (*B. nana*) have a higher ratio between the pollen grain diameter and the pore diameter than that of tree-birch pollen (*B. pubescens*). In this study, *B. nana* pollen is defined with a ratio larger than 10, while birch tree pollen is defined as smaller than 10. In total, nine samples between 425 and 632-cm depth (ca. 10 700–14 200 cal a BP) were analysed.

Sedimentary ancient DNA (sedaDNA)

In total, 191 samples have been analysed for *seda*DNA from cores 506-48 and 506-50. Further to the results presented in Clarke *et al*. (2019, 2020), we analysed 38 additional samples from the period 9500–15 000 cal a BP (380–708 cm, equal to zones BS2–BS4 in Clarke *et al*., 2020), which we combine with the original 25 samples to obtain 63 samples from this period. The extraction, polymerase chain reaction
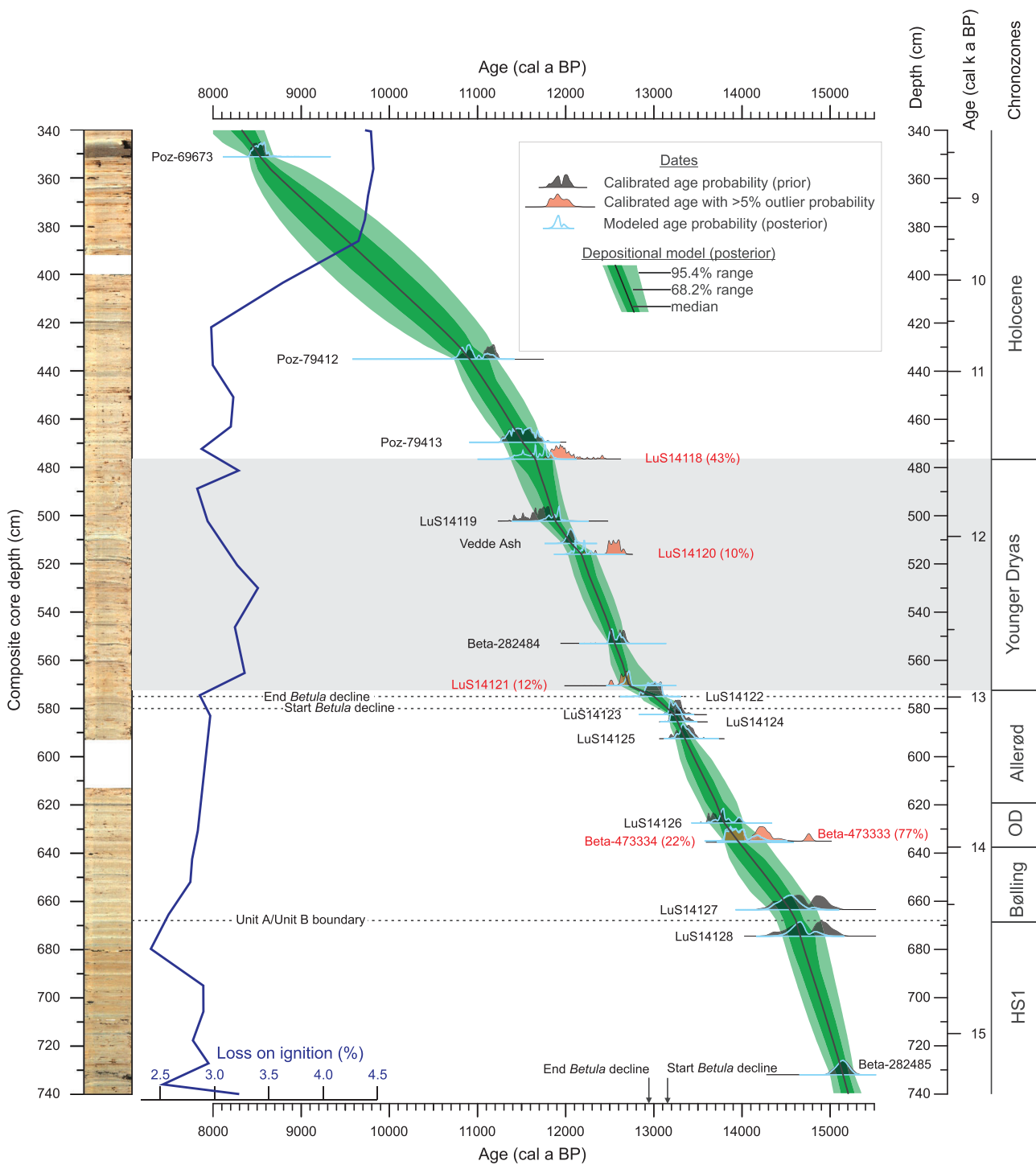
Figure 2. Lithostratigraphy (left column) and chronology of cores 506-48 and 506-50 from Lake Bolshoye Shchuchye used in this paper for the pollen and *sed*aDNA data. The age model is adapted from Regnéll *et al.* (2019) and Svendsen *et al.* (2019) with additional ¹⁴C dates. Details on radiocarbon dates are given in Haflidason *et al.* (this issue). The calibrated radiocarbon dates are plotted with 95% confidence intervals. The grey section highlights the YD period. Loss-on-ignition (LOI, %) is given in the blue curve on the left-hand side. Chronozones follow Mangerud (2021). [Color figure can be viewed at wileyonlinelibrary.com]

(PCR) amplification and sequencing follow Clarke *et al.* (2019), with the exception that the 38 additional samples analysed were extracted using the modified protocol presented in Rijal *et al.* (2020). DNA sequences retrieved from the 25 original samples were re-analysed, and the taxonomic assignment of all 63 samples covering the period 9500–15 000 cal a BP follows Rijal *et al.* (2020). In addition to the 35 negative controls (containing no sediment) that were analysed in Clarke *et al.* (2019, 2020), we analysed a further six negative extraction controls alongside the new samples analysed for this paper.

Each DNA extract and negative extraction control was independently amplified in eight PCR replicates using uniquely tagged generic primers that amplify the *trn*L P6 loop of the plant chloroplast genome (Taberlet *et al.*, 2007). To minimize any erroneous taxonomic assignments, only taxa with a 98% match, or greater, to a reference sequence were retained (Clarke *et al.*, 2020). We further removed sequences that displayed higher average reads in the negative extraction or PCR controls than in lake sediment samples. The taxonomic resolution varies according to the sequence variation within different taxa and is low for some families, for example

Poaceae and Salicaceae, and higher for others, for example Ericaceae, Saxifragaceae and Caryophyllaceae (Sønstebø et al., 2010).

sedaDNA data were visualized using the Tilia and TGView software (Grimm, 2011; tiliait.com). As for the pollen diagram, the sedaDNA diagram was subdivided into assemblage zones using CONISS (Grimm, 1987). The number of zones to use was determined by comparison with the broken-stick model as described for pollen data above.

Floristic richness

To estimate the floristic (palynological) richness, we rarefied the pollen and the sedaDNA data to estimate the number of terrestrial plant taxa that would have been detected if the count had been standardized among samples (Birks and Line, 1992). Rarefaction analysis was performed using the minimum count size in the vegan (Oksanen et al., 2017) package for R (R Core Team, 2017) for all samples in the period 9500–15 000 cal a BP. The minimum count size used for rarefaction in this paper was 26 691 DNA reads for sedaDNA samples and a $\Sigma P = 132$ terrestrial pollen and spores for pollen samples.

Compositional change

To reveal changes and/or variation in species assemblage composition and abundances, we performed a detrended correspondence analysis (DCA) on both the pollen and sedaDNA data using the vegan (Oksanen et al., 2017) package for R (R Core Team, 2017). We carried out a square-root transformation on the pollen and spore percentage data for terrestrial types before ordination, whereas no transformation was performed on the sedaDNA data. The sedaDNA data measure used for the DCA ordination was the proportion of PCR replicates per sample (out of eight).

Results

In total, 102 taxa were identified in the microfossil analysis (including indeterminable, unknown and Sphagnum spores) and 164 taxa in the sedaDNA for the period 15 000–9500 cal a BP. No new pollen or spore taxa were found after adding

samples, while 10 new sedaDNA taxa (Andreaea blytti, Andreaea nivalis, Aulacomnium palustre, Brachytheciastrum collinum, Chrysosplenium, Draba nemorosa, Encalypta, Geranium, Juniperus and Phalaris arundinacea) were recorded following the addition of new samples and/or re-analysis of the original dataset presented in Clarke et al. (2020). All data are shown in Tables S1–3.

CONISS cluster analysis revealed three distinct zones (BolS-1 to BolS-3) in the pollen and spore count data (Fig. 3, Fig. S2), their boundaries occurring at 672 and 485 cm (14 565 and 11 750 cal a BP). Cluster analysis failed to detect several other distinct changes in the pollen assemblages, including a major decrease in Betula pollen percentages between 572 and 485 cm. Thus, we further subdivided the pollen zone BolS-2 at 572 cm (12 800 cal a BP) into subzone 2a and 2b, based on visual inspection (Fig. 3).

CONISS cluster analyses based on sedaDNA proportion of reads and PCR replicates suggested three and four major zones, respectively (Fig. 4, Fig. S2). We use three cluster-defined zones (sedaDNA-1 to sedaDNA-3); these are congruent at a major division around 475 cm depth (11 610 cal a BP) and a secondary division at 614 cm depth (12 470 cal a BP). Non-significant subzones show where there are other major divisions in the cluster dendrogram. The major zone boundary at 475 cm (Fig. 4) is at the same level as the pollen zone boundary between BolS-2b and BolS-3 (Fig. 3). Cluster analysis and the zone boundaries in the two datasets are compared in Fig. S2. Outlines of the pollen and sedaDNA stratigraphy are described mainly according to the identified pollen assemblage zones with brief comments on vegetation development. As far as possible, the same taxa are used from both datasets in Figs. 3–5, which show selected taxa, while more complete data are presented in Figures S3–5. Figure 6 shows the estimated floristic (palynological) richness and diversity for both proxies.

Pollen and sedaDNA records during BolS-1 (15 000–14 565 cal a BP)

This zone starts below our present diagram (15 000 cal a BP) and lasts until 14 565 cal a BP. The microfossils are dominated by herbs (>70%) such as Artemisia, Chenopodiaceae,
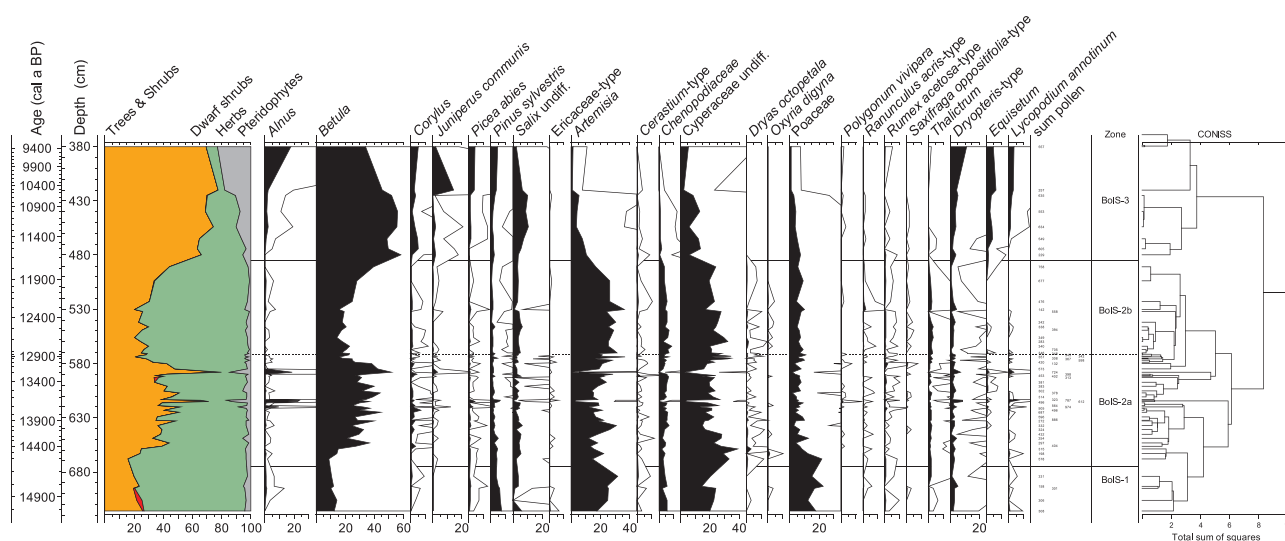

Figure 3. Summary pollen percentage diagram from Lake Bolshoye Shchuchye showing selected taxa over the time span 15 000–9500 cal a BP with pollen assemblage zones BolS-1 to BolS-3 indicated. Black silhouettes are the actual pollen percentages, and hollow silhouettes denote a 10× exaggeration of the percentage values. Total diagram with trees (orange), dwarf shrubs (red), herbs (green) and pteridophytes (grey). Samples are from cores 506-48 and 506-50. Pollen percentages are based on the sum of terrestrial pollen and spores. [Color figure can be viewed at wileyonlinelibrary.com]
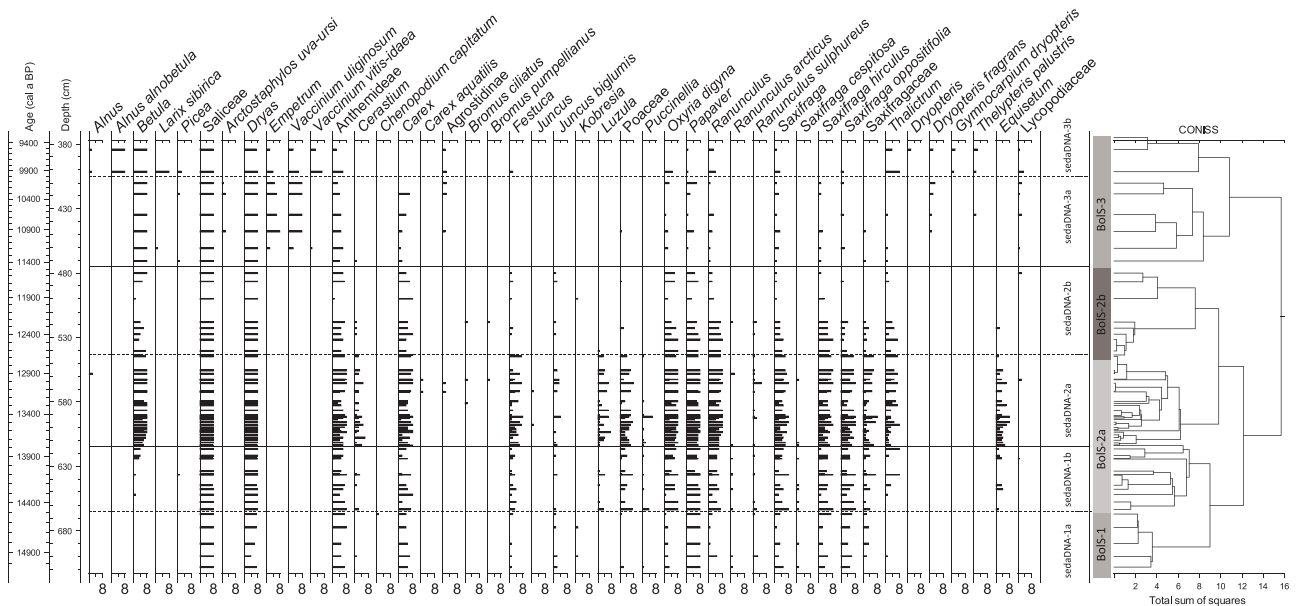
Figure 4. *sed*aDNA data from Lake Bolshoye Shchuchye for selected taxa. Histograms are taxa presented as a proportion of *sed*aDNA PCR replicates over the time span 15 000–9500 cal a BP with zone boundaries based on the *sed*aDNA data. Zone boundaries (BolS-1–3) from Fig. 3 are added for comparison. Samples are from cores 506-48 and 506-50.
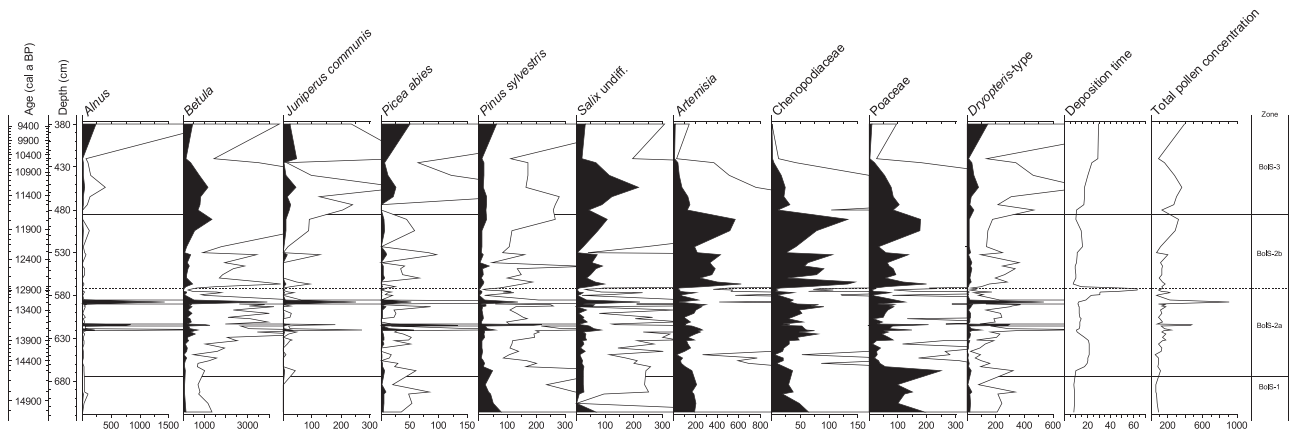

Figure 5. Pollen influx (accumulation rate) diagram for selected taxa from Lake Bolshoye Shchuchye plotted on the same age and depth scale and with the same pollen assemblage zones as in Fig. 3. Black silhouettes are the actual pollen influx values, and hollow silhouettes denote a 10× exaggeration of these. Sediment deposition time and total pollen concentration are given on the right.
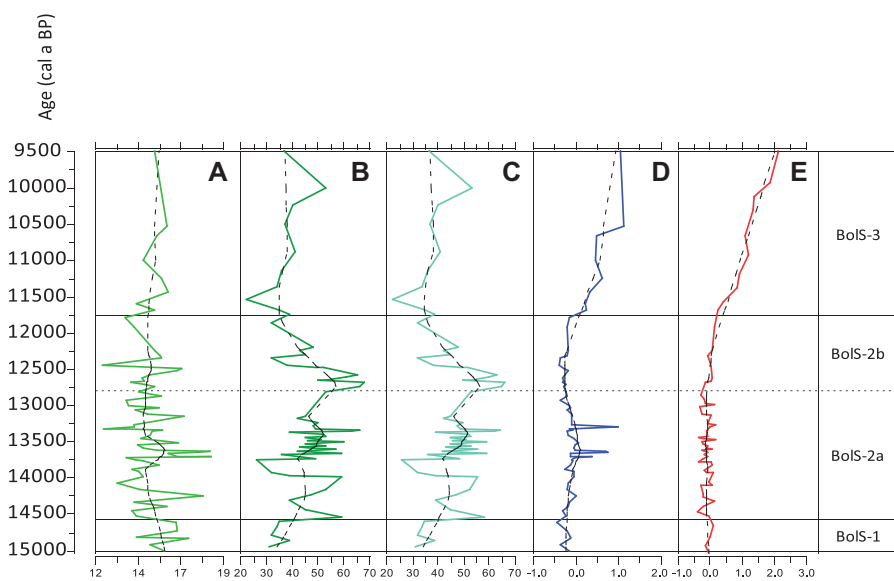

Figure 6. Measures of floristic richness (number of taxa per sample) based on *sed*aDNA and pollen from Lake Bolshoye Shchuchye from 15 000 to 9500 cal a BP based on pollen and spore data (A), pre-rarefaction (B) and post-rarefaction (C) of *sed*aDNA data, and detrended correspondence analysis (DCA) sample scores on axis I for pollen and spore data (D) and *sed*aDNA data (E). Smoothed curves are based on a LOESS smoother with span = 0.3 (black, dotted line). Pollen assemblage zones from Fig. 3 are indicated on the right. [Color figure can be viewed at wileyonlinelibrary.com]

Cyperaceae, Poaceae and *Rumex acetosa*-type (Fig. 3). Small amounts of fern (*Dryopteris*-type) and *Lycopodium annotinum* spores are present. Relatively low values of tree pollen (dominated by *Betula*, *Pinus* and *Picea*) are observed both in the pollen percentage (Fig. 3) and influx data (Fig. 5).

The data in *seda*DNA-1a are also dominated by herbs but include some shrub taxa (Fig. 4). Salicaceae and *Dryas*, along with herbaceous taxa such as Anthemideae, *Carex* and *Papaver*, occur in all eight PCR replicates in nearly all samples. *Oxyria digyna* and various *Saxifraga* species occur at lower levels of replication. No *seda*DNA sequences belonging to tree taxa were detected within this zone.

Rarefied floristic (palynological) richness for the microfossil data varies between 14 and 17 taxa, whereas rarefied floristic richness for *seda*DNA increases from 30 taxa at the start of this zone to up to 60 taxa towards the end of the zone (Fig. 6). According to the DCA sample scores on axis I for both pollen and *seda*DNA, the degree of compositional change in this zone is low (Fig. 6).

Pollen and sedaDNA records during BolS-2a (14 565–12 800 cal a BP) and BolS-2b (12 800–11 750 cal a BP)

In subzone 2a, 40–50% of the total pollen content is from trees (mainly *Betula*, but also *Alnus*, *Corylus*, *Picea* and *Pinus*). The percentage values of *Betula* are high, but the influx values are low, fluctuating between 100 and 350 pollen grains $cm^{-3} a^{-1}$. In this subzone, three short-lived peaks are observed in *Alnus* pollen percentages and influx values (at 13 660, 13 630, and 13 290 cal a BP). *Betula* influx values peak in the same levels. Above these *Alnus* peaks, there appear to have been periods with a somewhat higher sedimentation rate (Fig. 5). In BolS-2a, *Salix* undiff. pollen is present, but in low amounts. There are relatively high percentage values for *Artemisia*, Chenopodiaceae and Cyperaceae. *Dryas octopetala*, *Rumex acetosa*-type, and spores of *Dryopteris*-type and *Lycopodium annotinum* are also present. Pollen from aquatic plants occur mostly within BolS-2a. Single grains of *Menyanthes trifoliata*, *Nuphar* and *Sparganium*-type occur in one sample each, and *Potamogeton* and *Typha latifolia* are present in a few samples (Fig. S5). Total pollen concentration is higher in this zone than in BolS-1 with relatively high peaks observed at the same time as the *Alnus* pollen peaks. Seven of the nine samples with *Betula* pollen measurements belong to BolS-2a (Fig. 7).

The lower half of zone BolS-2a overlaps with the zone *seda*DNA-1b (14 570–13 620 cal a BP), whereas the upper part overlaps with *seda*DNA-2a (13 620–12 470 cal a BP) (Fig. 4, Fig. S2). In the *seda*DNA record, *Betula* increases from only being present in one PCR replicate in a few samples near the base of subzone BolS-2a to being consistently present in all eight PCR replicates of nearly all samples in the upper part of the subzone. These high values continue into subzone BolS-2b. Salicaceae remains the dominant woody taxon. Among the herbs, many of the taxa that were dominant in BolS-1 such as *Dryas*, Anthemideae, *Carex* and *Oxyria digyna* occur in this zone, and several *Saxifraga* taxa and *Papaver* remain dominant. *Equisetum*, *Cerastium*, *Festuca*, Poaceae, *Ranunculus* and *Saxifraga* taxa increase. The only aquatic plant taxa in the *seda*DNA record are *Caltha* and *Carex aquatilis* (two occurrences) on the boundary between subzones 2a and 2b.

At the base of BolS-2b, the pollen percentages for *Betula* decrease to below 20%. The one *Betula* pollen measurement in this subzone indicates that most of the pollen is from tree birch (Fig. 7). At the same time, herb pollen from *Artemisia* and Cyperaceae increases. Pollen from *Pinus sylvestris*, *Picea abies*, *Salix* undiff., *Dryas octopetala*, *Rumex acetosa*-type,
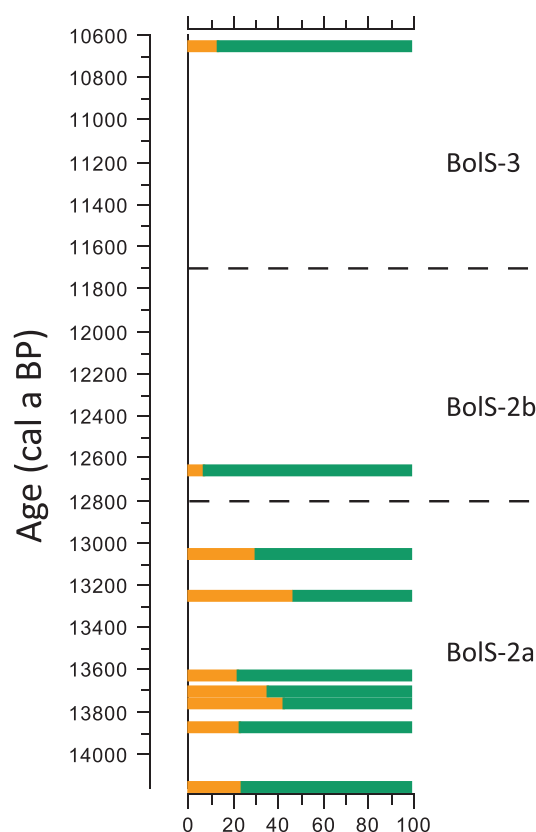

Figure 7. *Betula* pollen size (diameter/pore depth ratio) measurements – proportion of dwarf birch type (*B. nana*) in orange and tree birch type (*B. pubescens*) in green plotted as histogram bars indicating the sample positions. The age scale is the same as in Fig. 3. Pollen assemblage zones from Fig. 3 are indicated with dotted lines and zone names on the right. [Color figure can be viewed at wileyonlinelibrary.com]

Thalictrum, as well as *Dryopteris*-type spores are present throughout BolS-2b. Pollen influx values (Fig. 5) are generally low for the arboreal taxa and higher for the non-arboreal taxa. The total pollen concentration is relatively stable, with a slight increase towards the end of the subzone.

The boundary between pollen zones BolS-2a and BolS-2b (at 12 800 cal a BP, Fig. 3) falls within *seda*DNA-2a (13 620–12 470 cal a BP, Fig. 4). The taxonomic composition of *seda*DNA samples in the two subzones is relatively similar. Dominant taxa detected in many of the eight PCR replicates per sample are Salicaceae, *Dryas*, Anthemideae, *Carex*, Poaceae, *Oxyria digyna*, *Papaver*, *Ranunculus* and several *Saxifraga*-species. *Betula* is consistently present in all seven or eight PCR replicates per sample in *seda*DNA-2a (>2% of reads) and decreases to being present in one to five PCR replicates in *seda*DNA-2b (>0.01% from 12 470 to 11 610 cal a BP, Fig. 4).

The rarefied floristic (palynological) richness (Fig. 6) for both pollen and *seda*DNA data fluctuates frequently in zone BolS-2a. In BolS-2b, there is a gradual decrease, especially in the *seda*DNA data. The DCA axis scores are relatively constant throughout the two subzones. Small peaks occur in the pollen DCA coincident with the peaks in *Alnus* pollen percentages and influx in BolS-2a. In BolS-2b, the DCA axis scores are close to constant for both pollen and *seda*DNA data.

Pollen and sedaDNA records during BolS-3 (11 750–9500 cal a BP)

Zone BolS-3 represents about 2000 years in our selected period, and according to our age-model the zone starts at 11 750 cal a BP. At the end of BolS-2b and the onset of zone BolS-

3, marked increases occur in *Betula* pollen percentages and influx values at the same time as a marked drop in *Artemisia* pollen. For the sample at 10 660 cal a BP, *Betula* pollen sizes indicate that most pollen is of the tree-birch type. The total amount of tree pollen is above 60% in this zone. *Salix* undiff., *Picea abies* and *Alnus* pollen percentages increases slightly later. Influx values also increase from the start of this zone, as do values for total pollen concentration (Fig. 5). Values of the herb taxa that were abundant in BolS-2a and BolS-2b fall at the transition to BolS-3. *Dryas octopetala* pollen is no longer present. Spores of *Dryopteris*-type, *Equisetum* and *Lycopodium annotinum* increase.

The zonation of *seda*DNA data is marginally different from the pollen data, with the transition to *seda*DNA-3a at 11 610 cal a BP. The transition to this zone is characterized by the first appearance of several dwarf shrubs such as *Empetrum* and *Vaccinium uliginosum* and the fern *Dryopteris fragrans*. At the transition to *seda*DNA-3b, around 10 110 cal a BP, *Alnus* first appears and rapidly reaches >20% of the DNA reads (Table S3). Also, the dwarf shrubs *Vaccinium vitis-idaea* and *Rhododendron*, the forbs *Myosotis arvense* and *Alchemilla*, and the fern *Gymnocarpium dryopteris* appear. Some taxa that are scattered or common throughout the record, such as *Carex*, *Draba*, *Saxifraga hirculus* and *Eritrichium*, disappear, and *Dryas* percentages decrease to <5%. *Salix* is still dominant throughout BolS-3/*seda*DNA-3, and *Betula* shows a marked increase from just below this zone, reaching up to 24% of the DNA reads (Fig. 4). Rarefied floristic (palynological) richness based on pollen increases slightly from zone BolS-2b to BolS-3, whereas a slight decrease occurs in both pre- and post-rarefied richness for the *seda*DNA data in the beginning of the zone. There is a distinct increase in DCA axis I scores from the start of this zone through to the end in both datasets (Fig. 6).

Discussion

Vegetation change around Lake Bolshoye Shchuchye pre-Bølling–Allerød

This time window encompasses a dynamic period of climate and vegetation change: the transition out of latest glacial conditions into the Bølling through to the beginning of the warm early Holocene. The source area for the sediments and incorporated organic matter in Lake Bolshoye Shchuchye is large; the hydrological catchment is ca. 215 km^2 and hence the lake receives considerable inputs via the river and/or inwash events. Before 14 565 cal a BP there is a low abundance of tree pollen and, except for Salicaceae, woody taxa are absent from the *seda*DNA. The vegetation during this period was dominated by herb taxa belonging to arctic tundra and xeric steppe elements (*Papaver*, *Saxifraga*, *Kobresia*, *Artemisia*, Chenopodiaceae) characteristic of a cold and dry climate (Andreev *et al.*, 2001; Svendsen *et al.*, 2014). Relatively low values for rarefied floristic richness during this period, especially in the *seda*DNA record, support the inference of species-poor vegetation.

Start and development of the Bølling–Allerød

In western Europe, the start of the Bølling is generally considered to represent an abrupt warming. In the Greenland ice core chronology (GICC05) the onset is defined as 14 692 b2k (Rasmussen *et al.*, 2006), corresponding to 14 642 cal a BP. In lake sediments from western Europe, the start of the Bølling is identified by an increase in pollen from more warmth-demanding plants, often *Betula* (Krüger and Damrath, 2020). At Gerzensee (Ammann *et al.*, 2013), the Early Bølling is

associated with an increase in *Juniperus* and *Betula* pollen, and is dated to 14 665–14 443 cal a BP.

At Lake Bolshoye Shchuchye, a marked increase in total tree pollen, mainly driven by increasing *Betula* pollen percentages, takes place at the start of pollen zone BolS-2a (starting at 14 565 cal a BP, Fig. 3). The same timing marks the onset of zone *seda*DNA-1b (14 570 cal a BP); only occasional reads of *Betula* are recorded in the *seda*DNA at this point and the other woody taxa are Salicaceae and *Dryas*. At this time, however, many new herbaceous species appeared, suggesting climate warming (Fig. 4). Taking the age model at face value, there is a minor delay compared to the timing in Greenland and western Europe mentioned above, but the 95% confidence interval of our starting age for BolS-2a overlaps with the accepted start of the Bølling. In the *seda*DNA record, *Betula* appears slightly later than *Betula* pollen (Fig. 4), which may suggest that initially the pollen blew in from adjacent areas. From 13 730 cal a BP, however, *Betula* becomes continuously present in up to eight PCR replicates in nearly all *seda*DNA samples (Fig. 4), suggesting its local growth (Sjögren *et al.*, 2017; Alsos *et al.*, 2018).

Another record collected at a different point in the lake (Lenz *et al.*, this issue) shows an increase in pollen identified to *Betula* sect. *Nanae*. The increases in *Betula* are taken to reflect warmer conditions. Svendsen *et al.* (2014) infer summer temperatures between 6 and 8 °C for this period, which encompass the current conditions (7 °C). Rising summer temperatures are also supported by a chironomid-based temperature reconstruction (Lenz *et al.*, this issue). The warming is also registered as the complete disappearance of glaciers in the watershed of Lake Bolshoye Shchuchye at 14 350 cal a BP (Regnéll *et al.*, 2019) and by the onset of permafrost thaw in the Pechora Lowland, although the latter is not as precisely dated (Henriksen *et al.*, 2003). The appearance of pollen from several aquatic plant taxa in the lake, including *Typha*, also suggest warmer growth conditions. Enriched hydrogen isotope values derived from long-chain leaf waxes indicate greater locally derived summer precipitation that may reflect an increase in summer precipitation at our study site (Cowling *et al.*, this issue). This was possibly caused by reduced sea-ice cover in the Barents–Kara Sea and/or by increased transpiration from greater plant biomass. We conclude that within dating errors, a warming, possibly associated with increased moisture levels, started in the Polar Urals simultaneously with the onset of the Bølling in western Europe.

While tree-birch populations almost certainly were expanding regionally, tree-birch pollen influx at the site reached values higher than 250–300 grains cm^{-2} a^{-1} during zone BolS-2a (Fig. 5). Based on influx limits set by Hicks (2001) and the pollen-size measurements, it is conceivable that tree birches were locally present in favourable locations, probably together with dwarf birch (*B. nana*), which may have been more widely distributed. At other sites in the Polar Urals and adjacent lowlands, a similar increase in *Betula*, probably *B. nana*, is observed at about the same time, but a lack of robust age-models and/or lower sampling resolution makes precise correlations impossible (Paus *et al.*, 2003; Henriksen *et al.*, 2003; Andreev *et al.*, 2006; Svendsen *et al.*, 2014).

The short-lasting but distinct peaks in the *Alnus* pollen percentages in BolS-2a are not accompanied by any *Alnus* *seda*DNA (note that the corresponding *seda*DNA sample was only available for the sample at 13 631 cal a BP, Tables S2 and S3), suggesting that the *Alnus* peaks reflect local short-term peaks of *A. viridis* pollen or an increase in long-distance transported pollen. There is nothing in the sedimentary archive that indicates a hiatus or slumping of sediments during these

events that would imply reworking. We speculate that the two short-lived maxima in arboreal pollen (Figs. 3 and 5) may be linked to regional responses to oscillating temperatures during the Allerød chronozone found, for example, in Greenland ice-core records (Rasmussen *et al.*, 2006). This interpretation is supported by the occurrence *seda*DNA of the boreal taxa Lamiaceae, *Linum*, and *Lythrum salicaria* in the sample at 13 631 cal a BP, the latter two only observed in this sample (Tables SI2–3).

A surprising Betula decline 300 years before the onset of the YD

A typical response to the YD cooling in western Europe is a marked decline in *Betula* pollen simultaneous with an increase in *Artemisia* (Theuerkauf and Joosten, 2012). Having discovered a surprisingly early *Betula* decline in the original record (Clarke *et al.*, 2020), we dated more samples from this time interval. We can now precisely date the start and end of the *Betula*-pollen decline to 13 150 and 12 990 cal a BP, respectively (Fig. 8). Similarly, the percentage of *seda*DNA reads of *Betula* decreased between 13 200 and 12 500 cal a BP and reached a minimum at 11 860 cal a BP (Table S2); this may indicate a relative decrease in biomass in the catchment. However, *Betula* was consistently detected in eight repeats of all *seda*DNA samples of this period, which is consistent with its persistence in the catchment area. We interpret the strong decrease in *Betula* pollen and associated increase in pollen of *Artemisia* and other herbs to be a response to a cooling climate, which is the traditional interpretation in Europe. Without the enhanced set of ^{14}C ages and a high number of pollen samples we would certainly have postulated that the *Betula* decline showed the onset of the classic YD, but this explanation is now ruled out. In Fig. 8 we compare the timing of the *Betula* curve from Lake Bolshoye Shchuchye with features from some other key sites plotted on the same time scale and based on IntCal20 (Reimer *et al.*, 2020). These are the NGRIP δ^{18}O curve (Rasmussen *et al.*, 2006; Seierstad *et al.*, 2014), the marked decline in *Betula* (Birks and Birks, 2008, 2014; Bjune *et al.*, 2010), the lithological boundary at Kråkenes (Lohne *et al.*, 2014) and the Seso δ^{18}O curve (Cheng *et al.*, 2020). All records show the onset of the YD about 300 years later than the *Betula* decline in Lake Bolshoye Shchuchye.

There are several possible explanations for the early *Betula* decline and inferred cooling at Lake Bolshoye Shchuchye. The first is that the YD cooling started earlier in north-western Siberia than in western Europe, which would imply that the cooling propagated from Siberia westwards, or at least that there was a sizeable event in the Kara-Barents region that overprinted the North Atlantic signal. This could, for example, have been brought about through freshwater input into the eastern Arctic Ocean (Spielhagen *et al.*, 2005; Murton *et al.*, 2010; Condron and Winsor, 2012; Keigwin *et al.*, 2018; Condron *et al.*, 2020), leading to the formation of more sea ice. Subsequently sea ice and cold water may have been transported towards and through the Fram Strait (Tarasov and Peltier, 2005; Hillaire-Marcel *et al.*, 2013). The *seda*DNA record is far more stable. It shows a more local vegetation signal than the pollen and there is no clear shift when *Betula* pollen declines, but a cooler interval is indicated from 12 470 to 11 610 cal a BP. During this interval there is less consistent detection of *Betula* and the decrease or disappearance of many taxa (Tables S2 and S3).

A second explanation for the early *Betula* decline is that the vegetation reacted to the inter-Allerød cooling at about 13 100 cal a BP (Rasmussen *et al.*, 2006) and did not recover
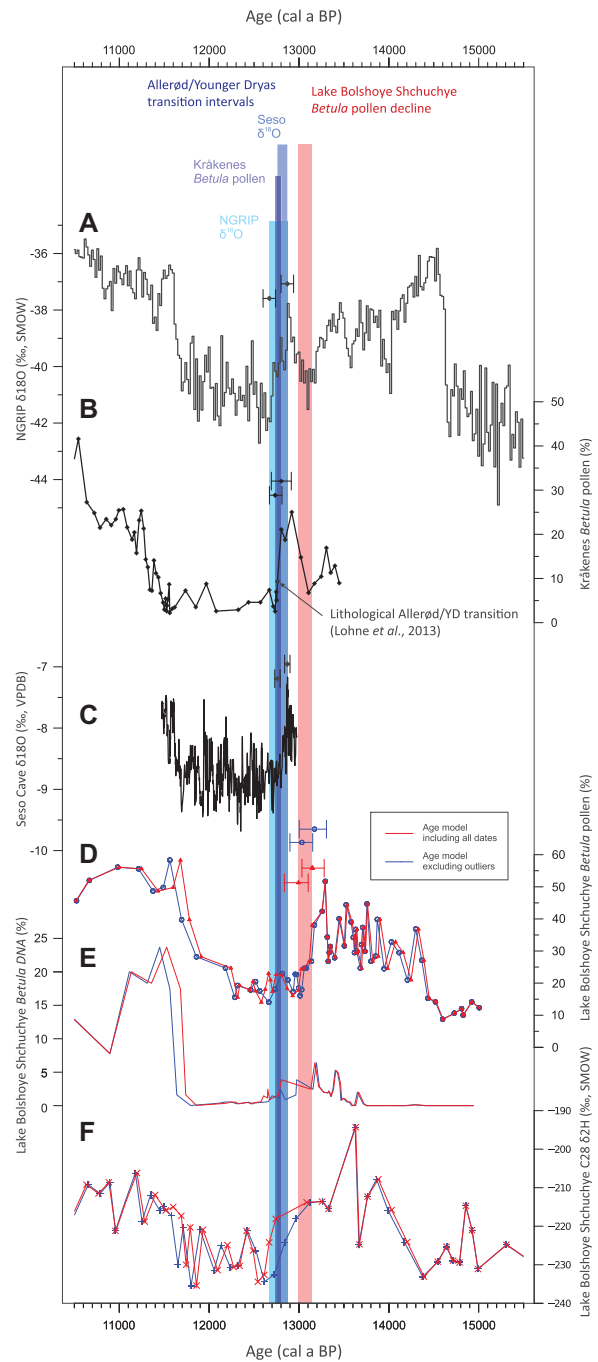

Figure 8. *Betula* pollen and *seda*DNA percentage data from Lake Bolshoye Shchuchye on two alternative age models (Fig. S1) (D, E, lower part) compared to: (A) NGRIP δ^{18}O (Seierstad *et al.*, 2014), (B) *Betula* pollen percentage from Kråkenes (Birks and Birks, 2008, 2014; Bjune *et al.*, 2010), (C) Seso cave δ^{18}O (Cheng *et al.*, 2020), and (F) measured *n*-alkanoic acids from Lake Bolshoye Shchuchye – C28 δ^2H (‰, SMOW) (Cowling *et al.*, this issue). [Color figure can be viewed at wileyonlinelibrary.com]

during the short-lived warming before the YD. This latter hypothesis is supported by leaf-wax hydrogen isotope (δ^2H) values that record summer precipitation δ^2H (Fig. 8) from the same core as our pollen diagram (Cowling *et al.*, this issue). These show stepwise changes coinciding with the Allerød/YD and YD/Holocene boundaries, indicating a well-defined YD contemporaneous with the YD in western Europe, although the amplitude of change was smaller at Lake Bolshoye Shchuchye. As mentioned above, higher δ^2H values early in the Allerød probably reflect an increase in locally derived summer moisture. The two-step decrease in δ^2H values towards the

Allerød/YD boundary would indicate a reversal in moisture conditions. Possibly, under strongly continental climate conditions, the gradual fall in enrichment and hence local moisture that began before the YD chronozone may have had a significant impact on conditions for tree growth (a threshold was crossed; Fig. 8). The trends in δ^2H values are consistent with *Betula pubescens* approaching Lake Bolshoye Shchuchye early in the Allerød but not returning near the end, whereas the consistent detection of *Betula* in the *seda*DNA probably represents *Betula nana* still present in the catchment.

Finally, given the mountain-range location of the study site, it is conceivable that locally generated climate features triggered an early *Betula* decline that was largely disconnected from hemispheric events. The reduced (less consistent) signal of the YD eastward across Siberia (Binney *et al.*, 2009) may reflect a growing influence of local dynamics on individual records the further from the North Atlantic a site lies.

Vegetation and climate dynamics through the YD

To compare the events during the YD in Lake Bolshoye Shchuchye with the North Atlantic sequence is challenging. For example, terrestrial proxy records suggest that the YD had two phases: a cold phase followed by a climatically more favourable phase, and that these changes were locally abrupt but also time-transgressive across Europe (Lane *et al.*, 2013). Our *seda*DNA shows the opposite pattern, with a warmer phase from 13 620 to 12 470 cal a BP, followed by a colder phase until 11 610 cal a BP. Furthermore, both influx and relative pollen values of *Betula* start to rise several centuries before the end of the YD.

The YD at Lake Bolshoye Shchuchye was characterized by a cold, dry climate steppe vegetation with *Artemisia*, Chenopodiaceae and Poaceae. Even dwarf shrubs declined and taxa typical of steppe increased in abundance (*Artemisia* and Chenopodiaceae). *seda*DNA of Anthemideae, which can potentially represent *Artemisia*, and the salt-tolerant grass *Puccinellia* also suggest dry conditions. All this suggests harsh conditions for woody taxa compared with the preceding interval. Co-dominance of tundra and steppe elements is observed in the pollen data from most other sites in the region (Andreev *et al.*, 1997, 2003, 2004; Khotinsky and Klimanov, 1997; Paus *et al.*, 2003; Väliranta *et al.*, 2006; Henriksen *et al.*, 2008; Svendsen *et al.*, 2014). Borisova (1997) infers that YD January temperatures in European Russia were about 1 °C lower than today, and about the same as today in July based on fossil pollen. The chironomid-based temperature reconstruction of Lenz *et al.* (this issue) indicates about 1.5 °C lower summer temperatures than today during the YD. Leaf-wax δ^2H data from the same cores as our pollen record suggest a return to more distal moisture sources, perhaps like conditions during the LGM (Cowling *et al.*, this issue). Haflidason *et al.* (2019b) suggest the lower sedimentation rate during the YD at Lake Bolshoye Shchuchye indicates low glacial activity during this interval, which was probably a function of low precipitation. Given the relatively small temperature decreases described above, we conclude that aridity probably affected the vegetation composition as much as temperature.

Presence of trees in the Polar Urals at the start of the Holocene

The transition into the Holocene is seen in the distinct rise in tree pollen percentages, mainly driven by *Betula*, together with a decrease in *Artemisia*, Cyperaceae and Poaceae. *Dryas octopetala* pollen disappears, but *Dryas* is still present in the *seda*DNA record. As plant macrofossils are lacking in our cores, the pollen influx together with the *seda*DNA are the best tools to determine if trees were present (Hicks and Hyvärinen, 1999; Hicks, 2001; Bjune, 2005). *Betula* influx values start to rise before the beginning of BolS-3 at 11 900 cal a BP, and reach >500 pollen cm^{-3} a^{-1}, which suggests the presence of birch trees in the catchment. This coincides with a marked increase in the proportion of *Betula seda*DNA reads (Fig. 4). The early Holocene peak in *Betula* pollen is followed by increases in *Alnus*, *Juniperus*, *Picea abies* and *Pinus sylvestris* pollen, suggesting that these trees were initially growing at some distance from the lake but managed to spread relatively fast when growing conditions improved. *Alnus* and *Larix sibirica* are consistently detected in eight *seda*DNA repeats per sample from 10 110 cal a BP, suggesting their presence within the catchment. *Picea* is also detected in the *seda*DNA record, but only in one or two repeats, which may be difficult to distinguish from background contamination (Alsos *et al.*, 2020). In addition to warmer conditions, the increase in pteridophyte spores (*Dryopteris*-type, *Equisetum*, *Lycopodium annotinum*) suggests increased moisture, both of which would have led to better growing conditions for trees. Clarke *et al.* (2020) provide a full description and discussion on tree immigration in the Holocene.

The presence of trees in possible refugial areas and resultant migration routes have always fascinated palaeoecologists. Recent publications using ancient DNA data and palaeoecological proxies indicate that the post-glacial immigration pattern for many plants is not as straightforward as first thought (Parducci *et al.*, 2012; Westergaard *et al.*, 2019; Alsos *et al.*, 2020). Biome reconstructions based on macrofossil records show that small populations of boreal trees gradually increased in their distribution from the onset of deglaciation at 17 000–18 000 cal a BP (Binney *et al.*, 2009; Tarasov *et al.*, 2009). Clarke *et al.* (2020) discuss whether *Picea* may have been present as (possibly ephemeral) populations at Lake Bolshoye Shchuchye during the full-glacial period, but their conclusion is equivocal. To date, data suggest that populations existed in the Western Siberian region, but no strong data place coniferous trees at Lake Bolshoye Shchuchye until the earliest Holocene, when a marked rapid increase in temperature provided suitable conditions for the local presence of trees.

Conclusions

Vegetation and climate reconstructions based on plant microfossil and ancient DNA (*seda*DNA) from Lake Bolshoye Shchuchye focus on the period from 15 000 to 9500 cal a BP. High-resolution data allow us to identify a warming in the Polar Urals that, within dating errors, is simultaneous with the onset of the Bølling in western Europe. This is evident mainly in the *Betula* proxy record, in which the pollen data respond earlier than the *seda*DNA data, the former probably reflecting changes on a regional scale, the latter local changes. Subsequently, the pattern of change from the Allerød interstadial into the Younger Dryas stadial does not entirely conform to the classic western European sequence; most notably there was a marked decline of *Betula* about 300 years earlier than the onset of the YD as dated in western Europe. New radiocarbon dates make it possible to date the start of the *Betula* decline precisely to 13 150 cal a BP and the end to 12 990 cal a BP. Furthermore, the greatest cooling observed during the YD appears to be the latter, rather than the initial part of the stadial, and aridity was probably high throughout. Possible explanations for the observed changes all draw to some degree on differences related to local or regional (i.e. Kara-Barents)

climate features that masked or overrode the main North Atlantic signal. Few records east of the Urals show the Lateglacial climate sequence in such detail. The results, which are chronologically secure, suggest that heterogeneous Lateglacial patterns might be expected eastward across Siberia.

Data availability statement

The forward and reverse raw DNA reads, along with the primer and tag sequence information, for all samples analysed as part of this paper will be made publicly accessible within the DRYAD database following acceptance of the manuscript for publication. The final *seda*DNA and pollen datasets that form the basis of the figures presented in this paper will be made available on the Neotoma Paleoecology Database at https://www.neotomadb.org/.

Supporting information

Additional supporting information can be found in the online version of this article.

Figure S1. The alternative age models for Lake Bolshoye Shchuchye used in this study. In blue the age model excluding outliers and in grey including all radiocarbon dates. Details on radiocarbon dates are given in Haflidason *et al.* (this issue). The calibrated radiocarbon dates are plotted with 95% confidence intervals. The grey section highlights the YD period. Loss-on-ignition (LOI) is given in the blue curve on the left side.

Figure S2. Comparison of dendrogram of a stratigraphical cluster (CONISS) analysis performed on the pollen and *seda*DNA records from Lake Bolshoye Shchuchye alongside the timing of zone boundaries assigned to the combined record.

Figure S3. Tree, shrubs and dwarf shrub taxa found in Lake Bolshoye Shchuchye over the period 15 000–9500 cal a BP. Blue silhouettes are the actual pollen percentages (p); hollow silhouettes denote a 10× exaggeration of the percentage values. Pollen percentages are based on the sum of terrestrial pollen and spores. Orange histograms are taxa presented as a proportion of *seda*DNA PCR replicates (DNA). Zone boundaries are pollen assemblage zones BolS-1 to BolS-3 as in Fig. 3. Samples are from cores 506-48 and 506-50.

Figure S4. Herb taxa found in Lake Bolshoye Shchuchye over the period 15 000–9500 cal a BP. Blue silhouettes are the actual pollen percentages (p); hollow silhouettes denote a 10× exaggeration of the percentage values. Pollen percentages are based on the sum of terrestrial pollen and spores. Orange histograms are taxa presented as a proportion of *seda*DNA PCR

replicates (DNA). Zone boundaries are pollen assemblage zones BolS-1 to BolS-3 as in Fig. 3. Samples are from cores 506-48 and 506-50. Part I – taxa from A–P, Part II – taxa from R–U.

Supporting information.

Figure S5. Pteridophytes and aquatic taxa found in Lake Bolshoye Shchuchye over the period 15 000–9500 cal a BP. Blue silhouettes are the actual pollen percentages (p); hollow silhouettes denote a 10× exaggeration of the percentage values. Aquatic pollen types are marked with a circle indicating presence. Pollen percentages are based on the sum of terrestrial pollen and spores. Orange histograms are taxa presented as a proportion of *seda*DNA PCR replicates (DNA). Zone boundaries are pollen assemblage zones BolS-1 to BolS-3 as in Fig. 3. Samples are from cores 506-48 and 506-50.

Table S1. All taxa pollen and spore taxa included in the pollen sum, given as counts given on a depth and age scale (cal a BP) together with the indication of the identified pollen zones (Fig. S2).

Table S2. All taxa identified by *seda*DNA shown as a percentage of total DNA reads per sample given on the depth and age scale (cal a BP) together with the identified sedaDNA zones (Fig. S2).

Table S3. All taxa identified by *seda*DNA shown as a percentage of total DNA reads per sample given on the depth and age scale (cal a BP) together with the identified *seda*DNA zones (Fig. S2).

Abbreviations. DCA, detrended correspondence analysis; CONISS, constrained cluster analysis on pollen percentage data by sum-of-squares; LGIT, Last Glacial–Interglacial Transition; LGM, Last Glacial Maximum; PCR, polymerase chain reaction; PFT, plant functional type; *seda*DNA, sedimentary ancient DNA; YD, Younger Dryas.

References

Alsos IG, Lammers Y, Yoccoz NG *et al.* 2018. Plant DNA metabarcoding of lake sediments: how does it represent the contemporary vegetation. *PLoS ONE* **13**: e0195403.

Alsos IG, Sjögren P, Brown AG *et al.* 2020. Last Glacial Maximum environmental conditions at Andøya, northern Norway; evidence for a northern ice-edge ecological "hotspot". *Quaternary Science Reviews* **239**.

Ammann B, van Leeuwen JFN, van der Knaap WO *et al.* 2013. Vegetation responses to rapid warming and to minor climatic fluctuations during the Late-Glacial Interstadial (GI-1) at Gerzensee (Switzerland). *Palaeogeography, Palaeoclimatology, Palaeoecology* **391**: 40–59.

Andreev AA, Forman SL, Ingólfsson Ó *et al.* 2006. Middle Weichselian environments on western Yamal Peninsula, Kara Sea based on pollen records. *Quaternary Research* **65**: 275–281.

Andreev AA, Manley WF, Ingólfsson Ó *et al.* 2001. Environmental changes on Yugorski Peninsula, Kara Sea, Russia, during the last 12,800 radiocarbon years. *Global and Planetary Change* **31**: 255–264.

Andreev AA, Nikolaev VI, Boi'sheiyanov DY *et al.* 1997. Pollen and isotope investigations of an ice core from Vavilov Ice Cap, October Revolution Island, Severnaya Zemlya Archipelago, Russia. *Géographie Physique et Quaternaire* **51**: 379–389.

Andreev AA, Tarasov PE, Klimanov VA *et al.* 2004. Vegetation and climate changes around the Lama Lake, Taymyr Peninsula, Russia during the Late Pleistocene and Holocene. *Quaternary International* **122**: 69–84.

Andreev AA, Tarasov PE, Siegert C *et al.* 2003. Vegetation and climate changes on the northern Taymyr, Russia during the Upper Pleistocene and Holocene reconstructed from pollen records. *Boreas* **3**: 484–505.

Bennett KD. 1996. Determination of the number of zones in a biostratigraphical sequence. *New Phytologist* **132**: 155–170.

Beug H-J. 2004. *Leitfaden der Pollenbestimmung für Mitteleuropa and angrenzende Gebiete*. München: Pfeil.

Binney H, Edwards M, Macias-Fauria M et al. 2017. Vegetation of Eurasia from the Last Glacial Maximum to present: key biogeographic patterns. *Quaternary Science Reviews* **157**: 80–97.

Binney HA, Willis KJ, Edwards ME et al. 2009. The distribution of late-Quaternary woody taxa in northern Eurasia: evidence from a new macrofossil database. *Quaternary Science Reviews* **28**: 2445–2464.

Birks HH, Birks HJB. 2014. To what extent did changes in July temperature influence Lateglacial vegetation patterns in NW Europe? *Quaternary Science Reviews* **106**: 262–277.

Birks HJB. 1968. The identification of *Betula nana* pollen. *New Phytologist* **67**: 309–314.

Birks HJB, Birks HH. 2008. Biological responses to rapid climate change at the Younger Dryas—holocene transition at Kråkenes, western Norway. *Holocene* **18**: 19–30.

Birks HJB. 1998. Numerical tools in palaeolimnology – progress, potentialities, and problems. *Journal of Paleolimnology* **20**: 307–332.

Birks HJB, Line JM. 1992. The use of rarefaction analysis for estimating palynological richness from Quaternary pollen-analytical data. *Holocene* **2**: 1–10.

Bjune AE. 2005. Holocene vegetation history and tree-line changes on a north–south transect crossing major climate gradients in southern Norway – evidence from pollen and plant macrofossils in lake sediments. *Review of Palaeobotany and Palynology* **133**: 249–275.

Bjune AE, Birks HJB, Peglar SM et al. 2010. Developing a modern pollen-climate calibration data set for Norway. *Boreas* **39**: 674–688.

Borisova OK. 1997. Younger Dryas landscape and climate in northern Eurasia and North America. *Quaternary International* **41–42**: 103–109.

Brendryen J, Haflidason H, Yokoyama Y et al. 2020. Eurasian Ice Sheet collapse was a major source of Meltwater Pulse 1A 14,600 years ago. *Nature Geoscience* **13**: 363–368.

Bronk Ramsey C. 2009a. Bayesian analysis of radiocarbon dates. *Radiocarbon* **51**: 337–360.

Bronk Ramsey C. 2009b. Dealing with outliers and offsets in radiocarbon dating. *Radiocarbon* **51**: 1023–1045.

Bronk Ramsey C, Lee S. 2013. Recent and planned developments of the program OxCal. *Radiocarbon* **55**: 720–730.

Bronk Ramsey CB. 2008. Deposition models for chronological records. *Quaternary Science Reviews* **27**: 42–60.

Cheng H, Zhang H, Spötl C et al. 2020. Timing and structure of the Younger Dryas event and its underlying climate dynamics. *Proceedings of the National Academy of Sciences of the United States of America* **117**: 23408–23417. [PubMed: 32900942]

Clarke CL, Alsos IG, Edwards ME et al. 2020. A 24,000-year ancient DNA and pollen record from the Polar Urals reveals temporal dynamics of arctic and boreal plant communities. *Quaternary Science Reviews* **247**.

Clarke CL, Edwards ME, Gielly L et al. 2019. Persistence of arctic-alpine flora during 24,000 years of environmental change in the Polar Urals. *Scientific Reports* **9**: 19613.

Condron A, Joyce AJ, Bradley RS. 2020. Arctic sea ice export as a driver of deglacial climate. *Geology* **48**: 395–399.

Condron A, Winsor P. 2012. Meltwater routing and the Younger Dryas. *Proceedings of the National Academy of Sciences of the United States of America* **109**: 19928–19933.

Fægri K, Iversen J. 1989. *Textbook of Pollen Analysis*. Wiley: New York.

Grimm EC. 1987. CONISS: a FORTRAN 77 program for stratigraphically constrained cluster analysis by the method of incremental sum of squares. *Computers and Geosciences* **13**: 13–35.

Grimm EC. 2011. TiliaIT: Tilia Software v. 2.6.1.

Haflidason H, Regnéll C, Pyne-O'Donnell S et al. 2019a. Extending the known distribution of the Vedde Ash into Siberia: occurrence in lake sediments from the Timan Ridge and the Ural Mountains, northern Russia. *Boreas* **48**: 444–451.

Haflidason H, Zweidorff JL, Baumer M et al. 2019b. The Lastglacial and Holocene Seismostratigraphy and sediment distribution of Lake Bolshoye Shchuchye, Polar Ural Mountains, Arctic Russia. *Boreas* **48**: 452–469.

Henriksen M, Mangerud J, Matiouchkov A et al. 2003. Lake stratigraphy implies an 80 000 yr delayed melting of buried dead ice in northern Russia. *Journal of Quaternary Science* **18**: 663–679.

Henriksen M, Mangerud J, Matiouchkov A et al. 2008. Intriguing climatic shifts in a 90 kyr old lake record from northern Russia. *Boreas* **37**: 20–37.

Hicks S. 2001. The use of annual arboreal pollen deposition values for delimiting tree-lines in the landscape and exploring models of pollen dispersal. *Review of Palaeobotany and Palynology* **117**: 1–29.

Hicks S, Hyvärinen H. 1999. Pollen influx values measured in different sedimentary environments and their palaeoecological implications. *Grana* **38**: 228–242.

Hillaire-Marcel C, Maccali J, Not C et al. 2013. Geochemical and isotopic tracers of Arctic sea ice sources and export with special attention to the Younger Dryas interval. *Quaternary Science Reviews* **79**: 184–190.

Hughes ALC, Gyllencreutz R, Lohne ØS et al. 2016. The last Eurasian ice sheets – a chronological database and time-slice reconstruction, DATED-1. *Boreas* **45**: 1–45.

Keigwin LD, Klotsko S, Zhao N et al. 2018. Deglacial floods in the Beaufort Sea preceded Younger Dryas cooling. *Nature Geoscience* **11**: 599–604.

Khotinsky NA, Klimanov VA. 1997. Allerød, Younger Dryas and early Holocene palaeo-environmental stratigraphy. *Quaternary International* **41–42**: 67–70.

Krüger S, Damrath M. 2020. In search of the Bølling-Oscillation: a new high resolution pollen record from the *locus classicus* Lake Bølling, Denmark. *Vegetation History and Archaeobotany* **29**: 189–211.

Lane CS, Brauer A, Blockley SPE et al. 2013. Volcanic ash reveals time-transgressive abrupt climate change during the Younger Dryas. *Geology* **41**: 1251–1254.

Lohne ØS, Mangerud J, Birks HH. 2014. IntCal13 calibrated ages of the Vedde and Saksunarvatn ashes and the Younger Dryas boundaries from Kråkenes, western Norway. *Journal of Quaternary Science* **29**: 506–507.

Mangerud J. 2021. The discovery of the Younger Dryas, and comments on the current meaning and usage of the term. *Boreas* **50**: 1–5.

Mangerud J, Andersen ST, Berglund BE et al. 1974. Quaternary stratigraphy of Norden, a proposal for terminology and classification. *Boreas* **3**: 109–126.

Mangerud J, Astakhov V, Svendsen J-I. 2002. The extent of the Barents-Kara ice sheet during the Last Glacial Maximum. *Quaternary Science Reviews* **21**: 111–119.

Mangerud J, Gosse J, Matiouchkov A et al. 2008. Glaciers in the Polar Urals, Russia, were not much larger during the Last Global Glacial Maximum than today. *Quaternary Science Reviews* **27**: 1047–1057.

Murton JB, Bateman MD, Dallimore SR et al. 2010. Identification of Younger Dryas outburst flood path from Lake Agassiz to the Arctic Ocean. *Nature* **464**: 740–743.

Muschitiello F, Wohlfarth B. 2015. Time-transgressive environmental shifts across northern Europe at the onset of the Younger Dryas. *Quaternary Science Reviews* **109**: 49–56.

Oksanen J, Blanchet FG & Friendly M et al. 2017. CRAN - Vegan: Community Ecology Package (r-project.org). version 2.4-2.

Parducci L, Jørgensen T, Tollefsrud MM et al. 2012. Glacial survival of boreal trees in northern Scandinavia. *Science* **335**: 1083–1086.

Paus A. 1988. Late Weichselian vegetation, climate, and floral migration at Sandvikvatn, North Rogaland, southwestern Norway. *Boreas* **17**: 113–139.

Paus A, Svendsen J-I, Matiouchkov A. 2003. Late Weichselian (Valdaian) and Holocene vegetation and environmental history of the northern Timan Ridge, European Arctic Russia. *Quaternary Science Reviews* **22**: 2285–2302.

R Core Team. 2017. *R: A Language and Environment for Statistical Computing*. R Foundation for Statistical Computing: Vienna.

Rasmussen SO, Andersen KK, Svensson AM et al. 2006. A new Greenland ice core chronology for the last glacial termination. *Journal of Geophysical Research* **111**.

Regnéll C, Haflidason H, Mangerud J et al. 2019. Glacial and climate history of the last 24 000 years in the Polar Ural Mountains, Arctic Russia, inferred from partly varved lake sediments. *Boreas* **48**: 432–443.

Reimer PJ, Austin WEN, Bard E et al. 2020. The IntCal20 northern hemisphere radiocarbon age calibration curve (0–55 cal kBP). *Radiocarbon* **62**: 725–757.

Rijal DP, Heintzman PD, Lammers Y et al. 2020. Sedimentary ancient DNA shows terrestrial plant richness continuously increased over the Holocene in northern Fennoscandia. *bioRxiv*.

Sadatzki H, Dokken TM, Berben SMP *et al.* 2019. Sea ice variability in the southern Norwegian Sea during glacial Dansgaard-Oeschger climate cycles. *Science Advances* **5**: eaau6174.

Seierstad IK, Abbott PM, Bigler M *et al.* 2014. Consistently dated records from the Greenland GRIP, GISP2 and NGRIP ice cores for the past 104 ka reveal regional millennial-scale $\delta^{18}O$ gradients with possible Heinrich event imprint. *Quaternary Science Reviews* **106**: 29–46.

Sjögren P, Edwards ME, Gielly L *et al.* 2017. Lake sedimentary DNA accurately records 20th century introductions of exotic conifers in Scotland. *New Phytologist* **213**: 929–941.

Sønstebø JH, Gielly L, Brysting AK *et al.* 2010. Using next-generation sequencing for molecular reconstruction of past Arctic vegetation and climate. *Molecular Ecology Resources* **10**: 1009–1018.

Spielhagen RF, Erlenkeuser H, Siegert C. 2005. History of freshwater runoff across the Laptev Sea (Arctic) during the last deglaciation. *Global and Planetary Change* **48**: 187–207.

Svendsen JI, Alexanderson H, Astakhov VI *et al.* 2004. Late Quaternary ice sheet history of northern Eurasia. *Quaternary Science Reviews* **23**: 1229e1271.

Svendsen JI, Haflidason H, Henriksen M *et al.* 2019. Glacial and environmental changes during the last 60,000 years in the Polar Ural Mountains, Arctic Russia, inferred from a high resolution lake record and observations from adjacent areas. *Boreas* **48**: 407–431.

Svendsen JI, Krüger LC, Mangerud J *et al.* 2014. Glacial and vegetation history of the Polar Ural Mountains in northern Russia during the Last Ice Age, Marine Isotope Stages 5–2. *Quaternary Science Reviews* **92**: 409–428.

Taberlet P, Coissac E, Pompanon F *et al.* 2007. Power and limitations of the chloroplast trnL (UAA) intron for plant DNA barcoding. *Nucleic Acids Research* **35**: e14.

Tarasov L, Peltier WR. 2005. Arctic freshwater forcing of the Younger Dryas cold reversal. *Nature* **435**: 662–665.

Tarasov PE, Bezrukova EV, Krivonogov SK. 2009. Late Glacial and Holocene changes in vegetation cover and climate in southern Siberia derived from a 15 kyr long pollen record from Lake Kotokel. *Climate of the Past* **5**: 285–295.

Tarasov PE, Leipe C, Wagner M. 2021. Environments during the spread of anatomically modern humans across Northern Asia 50–10 cal kyr BP: what do we know and what would we like to know? *Quaternary International* **596**: 155–170.

Theuerkauf M, Joosten H. 2012. Younger Dryas cold stage vegetation patterns of central Europe – climate, soil and relief controls. *Boreas* **41**: 391–407.

Väliranta M, Kultti S, Seppä H. 2006. Vegetation dynamics during the Younger Dryas–Holocene transition in the extreme northern taiga zone, northeastern European Russia. *Boreas* **35**: 202–212.

Westergaard KB, Zemp N, Bruederle LP *et al.* 2019. Population genomic evidence for plant glacial survival in Scandinavia. *Molecular Ecology* **28**: 818–832.